Experimental Mechanics (2012) 52:83–93
DOI 10.1007/s11340-011-9538-4

Effect of Facesheet Thickness on Dynamic Response of Composite Sandwich Plates to Underwater Impulsive Loading

S. Avachat · M. Zhou

Received: 19 May 2011 / Accepted: 22 August 2011 / Published online: 11 September 2011

Abstract The response of sandwich structures to underwater blast loading is analyzed. The analysis focuses on the effect of varying structural attributes on energy dissipation and deformation. The structures analyzed are planar sandwich plates with polymer foam cores and fiber-reinforced polymer composite facesheets. The thickness of the facesheets is varied under the conditions of constant material properties and core dimensions. The fully three-dimensional finite-element simulations carried out account for underwater blast loading through the use of the Mie-Gruneisen equation-of-state of a linear Hugoniot form and a modified Drucker-Prager core crushing model. The impulse imparted to the panels is varied from 4 to 42 kPa·s. The results show that there exists an optimal thickness of the facesheets which maximizes energy absorption in the core and minimizes the overall deflection of the structure.

Keywords Sandwich structures · Composites · Dynamic response · Underwater impulsive loading

Introduction

Ships, submersibles and other marine structures are susceptible to damage due to dynamic loading from underwater explosions, projectile impact and hull slamming resulting from high-speed motion. Composite structures for such marine structures are often designed with large safety factors which limit gains in speed and payload-carrying capacity. In recent years, sandwich structures with strong facesheets and lightweight cores have become central structural components of naval vessels which are required to be blast-resistant. The applications take advantage of the high strength-to-weight ratios, durability and low life-cycle costs of fiber-reinforced composites and polymeric foam cores. This emerging trend necessitates quantification of the responses of these structures as functions of constituent material behavior, structural hierarchy and complex loading conditions.

By virtue of the combination of a thick core and thin facesheets, sandwich structures achieve considerably high shear-stiffness-to-weight ratios and bending-stiffness-to-weight ratios than equivalent homogeneous plates made exclusively of the core material or the facesheet material. The primary factors that influence the structural response of a sandwich structure are (1) facesheet thickness, (2) core thickness and (3) core density. Zenkert [1] provided a review of the mechanics of sandwich structures, expanding on the previous work of Plantema [2] and Allen [3]. The bulk of previous research on the dynamic behavior of sandwich composites has focused on low-velocity contact-based loads such as drop weight and projectile impact [4–10]. Common failure modes that have been identified include core indentation and cracking, core shear, facesheet buckling and delamination, core-facesheet debonding and perforation. Experimental studies aimed at understanding material and structural responses under blast loads have been carried out. Studies on metallic sandwich panels subjected to air blasts [11, 12], indicate that sandwich plates with high-ductility and high energy absorption capacity per unit areal mass show good performance. Liang et al. [13] and Wei et al. [14] studied the behavior of metallic

S. Avachat · M. Zhou (✉)
The George W. Woodruff School of Mechanical Engineering,
School of Materials Science and Engineering,
Georgia Institute of Technology,
Atlanta, GA 30332-0405, USA
e-mail: min.zhou@gatech.edu

S. Avachat
e-mail: sidavachat@gmail.com

sandwich cores with varying strengths and found that "soft" cores reduce the momentum transferred, thus providing better mitigation for blast loading. For metallic structures, energy absorption in metallic lattice cores is through large-scale plasticity, shear and compressive buckling, and eventual tearing of core walls and facesheets. Tekalur and Shukla [15] examined the dynamic response of woven E-glass composite facesheets and stitched core sandwich structures to air-based shock loading and concluded that stitched cores exhibit superior mechanical performance. Espinosa et al. simulated underwater blasts by impacting a projectile on a piston in contact with water [16, 17] and concluded that steels may be preferred when maintenance of residual strength is a priority and composite materials make better low-weight blast-resistant hulls. The use of explosives to generate underwater impulsive loads has also been reported [18–20].

The core plays a very important role in determining the dynamic response of sandwich composites because it accounts for the largest fraction of the overall energy dissipated. Split-Hopkinson Pressure Bar apparatuses have been employed to measure the stress-strain behavior of PVC foams at high strain rates [21–23]. Experiments reveal that PVC foams have mild strain rate sensitivity in the strain rate range of $\dot{\varepsilon} = 10^{-2}$ to $10^{3}\ s^{-1}$ and negligible strain rate sensitivity rate in the strain rate range of $\dot{\varepsilon} = 10^{-4}$ to $10^{-2}\ s^{-1}$. The primary mechanism for energy absorption in foam cores is local wall collapse and volumetric compression. The facesheets play an important role in determining the shear and bending resistances and energy dissipation. The primary mechanisms for energy absorption and failure in fiber-reinforced composite facesheets are cracking, delamination, fiber breakage and fragmentation [24, 25]. While previous research in blast mitigation has focused on metallic sandwich structures, there is a need for further research in a number of areas, especially with regard to composite polymeric sandwich structures. In particular, the use of novel materials and configurations for enhanced blast mitigation capabilities, the response of facesheets under very high pressures and the response of structures under submerged conditions are some important issues yet to be explored and fully quantified.

The objective of this study is to examine the effect of the ratio between facesheet thickness and core thickness on the dynamic response of composite sandwich structures. To this end, the core thickness and core density are kept constant and the thickness of the facesheets is varied. Under this condition, the total mass of the structure changes with the thickness of the facesheets. Another approach is to keep the total weight constant and vary the thicknesses of the core and the facesheets accordingly. The second approach can lead to unrealistic sandwich designs and, therefore, is not followed here. We quantify the response of the structures using fiber and matrix damage, facesheet deflections and energy absorbed. The results are analyzed in both normalized and non-normalized forms to gain insight into underlying trends that can be explored in the design of materials and structures.

Experimental Configuration

Gas gun impact has been successfully used to generate impulsive loading through water [16, 26, 27]. To obtain controlled loading and simulate various water-structure contact scenarios, we have designed and fabricated an experimental facility which allows a variety of load configurations to be studied with quantitative diagnostics. Important features of this facility include the ability to generate water-based impulsive loading of a wide-range of intensities, the ability to simulate the loading of submerged structures, and integrated high-speed photographic and laser interferometric diagnostics. This facility is used in conjunction with computational modeling. Figures 1 and 2 show a picture of this facility and a schematic illustration of the experimental configuration analyzed in this paper. The shock tube is a 500 mm long cylinder which is horizontally mounted and filled with water. It is made of steel and has an inside diameter of 76 mm. A thin piston plate is mounted at the front (left) end and the specimen is located at the rear (right) end. A projectile is accelerated by the gas gun and impacts the piston plate, generating a planar pressure pulse in the shock tube. This pulse travels down the shock tube and impinges upon the specimen. The target is supported by an anvil which is bolted to an I-beam.

Depending on the projectile velocity, pressures ranging from 10 to 300 MPa can be generated in the shock tube. The cylindrical shape of the shock tube allows an essentially uniform pressure to be applied to the target over the area of contact. The temporal and spatial profiles of the pressure pulse depend on the materials of the projectile and the piston. Figure 3 shows the pressure histories corresponding to five different projectile velocities, as predicted by the simulations. These pressure measurements

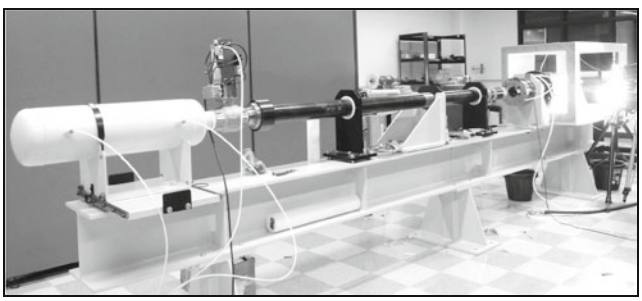

Fig. 1 Experimental facility for generating underwater impulsive loading on sandwich structures

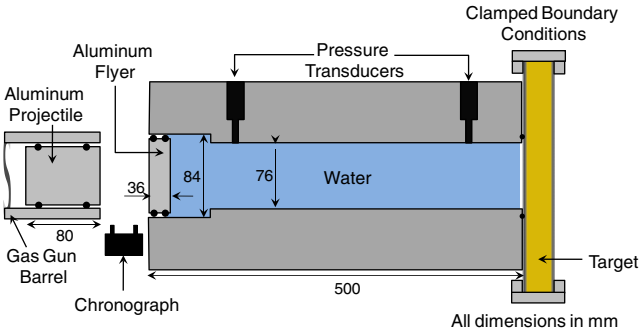

Fig. 2 Schematic illustration of experimental setup for underwater impulsive loading of a composite sandwich panel

are taken at a distance of 300 mm from the piston (the second pressure port shown in Fig. 2). The rise time of the pulses is on the order of 25 μs and the decay time is on the order of 250 μs. Impulse I is calculated as $I = \int p \cdot dt$, where p is the pressure, t is the decay time. The five impulse magnitudes considered in the simulations are 42, 30, 18, 12 and 4 kPa·s.

Materials

The core is made of Divinycell H-100 PVC foam [28] whose response is described by a volumetric hardening model in which the evolution of the yield surface is driven by the volumetric plastic strain. The stress-strain relation for the foam is shown in Fig. 4 [23]. The response consists of three distinct regimes: (1) nearly elastic initial deformation, (2) plateau region in which deformation occurs at relatively constant stress, and (3) lock-up/densification stage beyond which the material becomes fully compacted. The constitutive model adopted for Dinvinycell H100 PVC foam is the one developed by Zhang et al. [29] and implemented in the current finite element code [30, 31]. The model accounts for isotropic, dilatational plasticity. Studies on PVC foams show a weak dependence on strain rate [23]. Hence, the foam is assumed to be strain-rate independent in the current study.

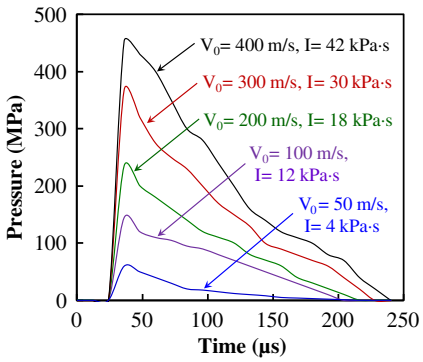

Fig. 3 Pressure profiles at different load intensities

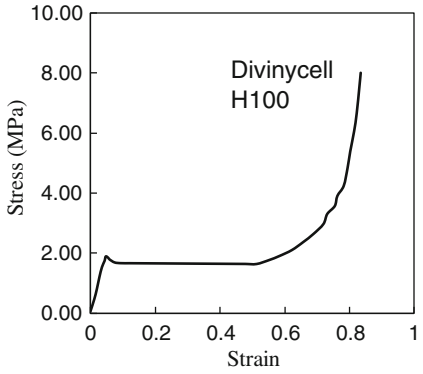

Fig. 4 Response of Divinycell H100 foam under quasi-static uniaxial compression [23]

The facesheets are made of a glass fiber reinforced epoxy composite. The facesheet thicknesses and corresponding areal masses of the structures are listed in Table 1. Each facesheet consists of plies in a bi-axial $[0/90]_S$ layup and is modeled with the Hashin damage model with energy-based damage evolution [32].

The damage initiation mechanisms considered for a transversely isotropic laminate include

(a) matrix tension damage as measured by the damage parameter

$$F_m^t = \left(\frac{\sigma_{11}}{X^T}\right)^2 + \left(\frac{\tau_{12}}{S^L}\right)^2, \quad (1)$$

(b) matrix compression damage as measured by

$$F_m^c = \left(\frac{\sigma_{22}}{2S^T}\right)^2 + \left(\frac{\tau_{12}}{S^L}\right)^2 + \left[\left(\frac{Y^C}{2S^T}\right)^2 - 1\right]\frac{\sigma_{22}}{Y^C}, \quad (2)$$

(c) fiber tension damage as measured by

$$F_f^t = \left(\frac{\sigma_{11}}{X^T}\right)^2 + \left(\frac{\tau_{12}}{S^L}\right)^2, \quad (3)$$

and

Table 1 Structural characteristics of sandwich configurations analyzed

Facesheet Thickness	Number of Plies [0/90]s (0.25 mm each)	T_f/T_c	Areal Mass of Entire Structure (kg/m^2)
1	4	0.05	8
2	8	0.1	12
3	12	0.15	16
6	24	0.3	28
8	32	0.4	36
12	48	0.6	52
15	60	0.75	64
20	80	1	84

(d) fiber compression damage as measured by

$$F_f^c = \left(\frac{\sigma_{11}}{X^C}\right)^2. \quad (4)$$

In the above expressions, σ_{11}, σ_{22}, and τ_{12} are components of effective stress tensor σ used to define the initiation criteria, X^T and Y^T are the longitudinal and transverse tensile strengths, X^C and Y^C are the longitudinal and transverse compressive strengths, S^L is the longitudinal shear strength and S^T is the transverse shear strength. The parameters used in the simulations can be found in Table 2.

The response of water is described by the Mie-Gruneisen equation of state of the linear Hugoniot form, or

$$p = \frac{\rho_0 {c_0}^2 \eta}{(1 - s\,\eta)^2}\left(1 - \frac{\Gamma_0 \eta}{2}\right) + \Gamma_0 \rho_0 E_m, \quad (5)$$

where p is the current pressure, c_0 is the speed of sound, ρ_0 is the initial density, E_m is internal energy per unit mass, Γ_0 is Grüneisen's Gamma at a reference state, $s = dU_s/dU_p$ is the Hugoniot slope coefficient, U_s is the shock wave velocity and U_p is the particle velocity which is related to U_s through the relation

$$U_S = c_0 + sU_p. \quad (6)$$

The values of the constants are listed in Table 3.

Table 3 Parameters for the Mie-Gruneisen equation of state for water

ρ_0	c_0	Γ_0	$s = dU_s/dU_p$
kg/m^3	m/s	(Dimensionless)	(Dimensionless)
980	1500	0.1	1.75

Structures Analyzed

The load configuration analyzed consists of a sandwich plate subject to impulsive loading at its center. The plate can be regarded as a portion of a ship's hull. The exponentially decaying pressure pulse has an impulse consistent with what is first proposed by Taylor [33]. Figure 5 shows a schematic illustration of a square sandwich plate 300×300 mm in size with a loading area of 76 mm in diameter at the center. The load area is 5% of the total area of the plate.

The outer boundaries of the plate are clamped. The symmetries of the plate and loading allow a quarter of the total plate to be considered in the simulations. All panels have a core thickness of T_c=20 mm and a core density of ρ_c=100 kg/m^3, giving a core unit areal mass of M_c=2 kg/m^2. The side length of the plate is L=300 mm. The facesheets, consisting of plies 0.25 mm in thickness each, are modeled with continuum shell elements. The total facesheet thickness T_f varies from 1 to 20 mm, giving rise to different areal mass values of the sandwich plates. The ratio between the facesheet thickness and the core thickness is $R=T_f/T_c$. All plates have the same material properties. Figure 6(a–d) illustrate the sandwich plates analyzed, the T_f/T_c value ranges from 0.05 to 1. The insets show magnified views of the plates. In the simulations, the plates are considered to be free of defects due to manufacturing variability or pre-stress.

Finite Element Model

The numerical model explicitly accounts for the projectile, piston plate and water column in contact with the sandwich plate target. The projectile is prescribed with an initial velocity V_0. Simulations are carried out with a Lagrangian description for the water and target. Since the Lagrangian framework produces water-structure interactions and accurate pressures and impulses, we use this framework for the current set of calculations.

Table 2 Material parameters for facesheets and core

	Unit	Glass Fiber Epoxy [35]	Divinycell H100 [28]
Density	kg/m^3	2100	100
Tensile Modulus [E_x]	MPa	44000	130
Transverse Modulus [E_y]	MPa	9000	135
Shear Modulus [G_{xy}, G_{xz}, G_{yz}]	MPa	4000	35
Longitudinal Tensile Strength	MPa	2500	3.5
Longitudinal Compressive Strength	MPa	2000	2
Transverse Tensile Strength	MPa	75	3.5
Transverse Compressive Strength	MPa	150	2
Longitudinal Shear Strength	MPa	75	1.6
Transverse Shear Strength	MPa	75	1.6

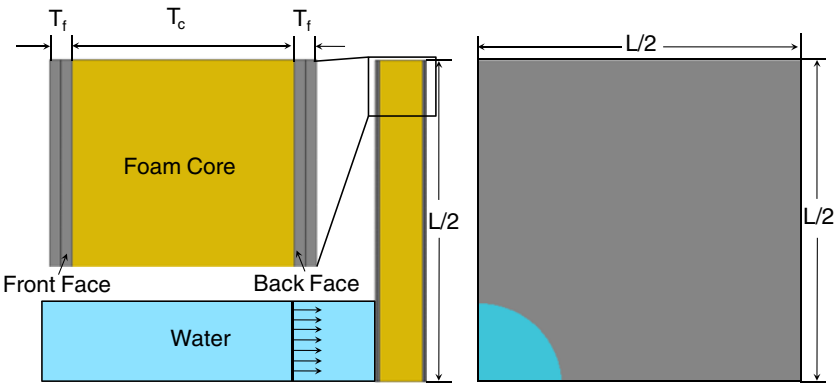

Fig. 5 Configuration of planar sandwich structures subject to water-based impulsive loads

The projectile, piston, water and foam core are discretized with 8-node 3D brick elements while the composite facesheets are discretized with continuum shell elements. A $[0/90]_S$ layup is specified for each ply in the facesheets. For the composite material of the facesheets, an element is deleted if internal damage exceeds a pre-determined threshold. A master-slave contact algorithm is used for interactions between the facesheets and core and a non-penetrating, general contact algorithm is implemented at projectile-piston, piston-water and water-sandwich structure interfaces. Cohesive elements are used at the core-facesheet interfaces to simulate core-facesheet debonding [30, 34]. A bilinear cohesive law is implemented, accounting for mixed-mode failure at the interfaces. A normal penalty-based contact algorithm is used to prevent interpenetration of crack surfaces. Figure 7 shows a side-view of the quarter symmetry finite element model with mesh refinement at the interfaces. The following quantities are tracked to quantify and compare the responses of the sandwich plates:

(a). The displacements at the center of facesheets 1 and 2;
(b). Core crushing rate and core crushing strain;
(c). Energy dissipated in the structure; and
(d). Compressive and tensile damages in the facesheets.

When an explosive detonates in a marine environment, the expanding chemical products compress the surrounding water and propagate outwards at high velocities. The shock wave can be described by the Rankine-Hugoniot jump equations which are derived from the conservation of mass, momentum and energy. At any distance from the point source, the blast pressure exponentially decays over time. Underwater blasts are much more harmful than air blasts because the impedance mismatch between water and sandwich structures is smaller than that between air and sandwich structures. Also, underwater blast waves propagate farther and maintain their magnitude over larger distances than air blast waves. At any point, the pressure history can be characterized by

$$p(t) = p_0 \exp\left(-\frac{t}{\theta}\right), \tag{7}$$

where p_0 is the peak pressure, t is time and θ is the decay constant.

Different values of peak pressure and decay constant are obtained by varying the initial velocity of the projectile. Apart from the projectile velocity, other factors that influence the pressure pulse are projectile mass, piston plate thickness, and the shape of the shock tube. All

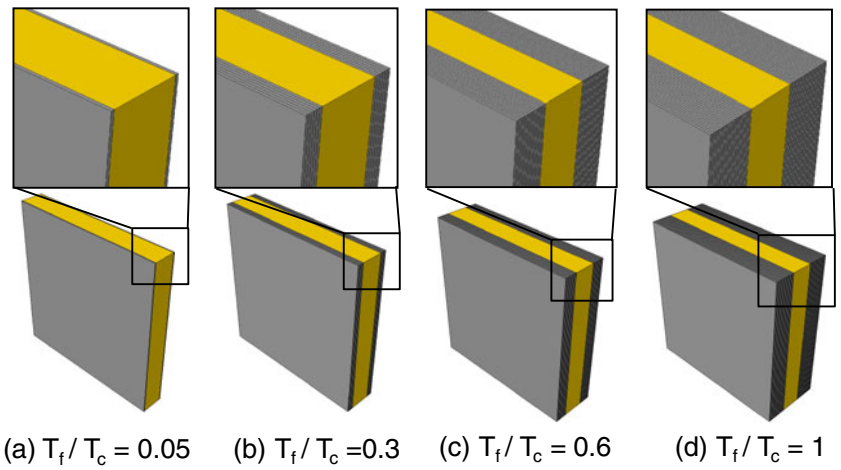

Fig. 6 Configurations of composite sandwich structures with different facesheet thicknesses

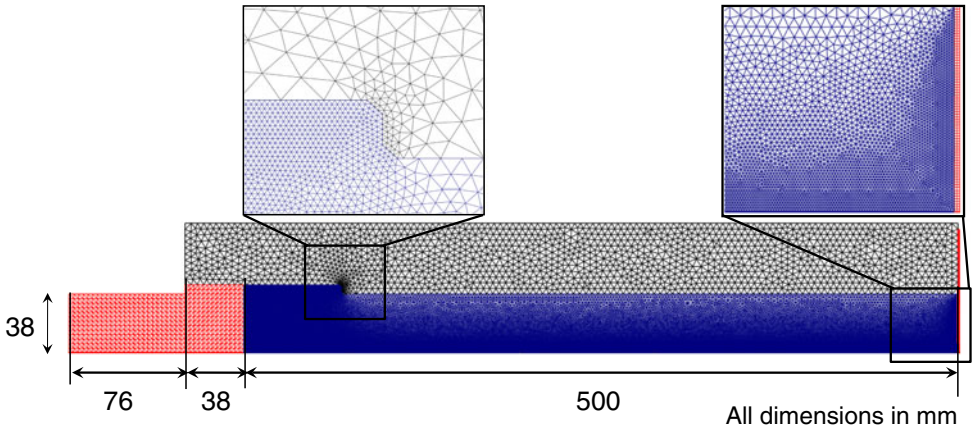

Fig. 7 Side-view of quarter-symmetric finite element mesh for water-structure model

variables are varied to obtain impulses that best match analytical predictions from the Taylor analysis [33]. The pressure decays faster in the numerical data largely due to higher dissipation rates in the finite element description. Hence, the parameters in the equation of state for water are adjusted to obtain close matches between the numerical and analytical results.

Results

To illustrate the process at hand, Fig. 8 shows the distribution of particle velocity at different times after the projectile comes into contact with the piston. The projectile velocity is 200 m/s (giving rise to an impulse of I= 18 kPa·s). The particular sandwich structure has thickness ratio of T_f/T_c=0.05. The velocity is relatively uniform across the cross-section of the shock tube and the reflection of the pulse from the water-target interface can be seen. Cavitation occurs at the water-target interface when the pressure drops to zero.

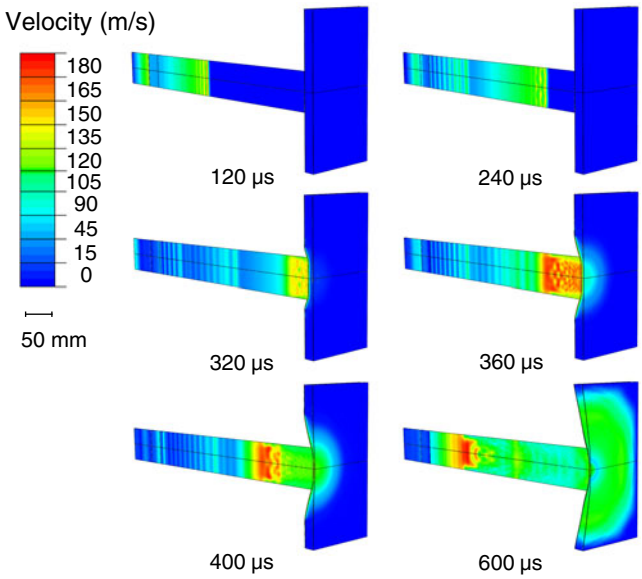

Fig. 8 Sectional views of an impulsive loading process obtained by three-dimensional finite element simulation. The sequence of images show the distributions of particle velocity at different times. The impulsive loading intensity is I=18 kPa·s

A large number of calculations have been carried out. The deformation of the core shows three distinct stages of response: (1) onset of core crushing, (2) onset of motion of back face and (3) momentum transfer through the structure. Changes made to the facesheets affect all three stages. In general, all things being equal, structures with thicker facesheets are stronger in an absolute sense, since more material is used. To reveal trends on a per weight basis, we analyze the results in both normalized and non-normalized forms.

For the five impulse levels per unit area considered (I= 4 kPa·s, I=12 kPa·s, I=18 kPa·s, I=30 kPa·s and I= 42 kPa·s), we first focus on the results for I=18 kPa·s and then compare the results for the different impulse levels. Facesheets with thicknesses less than 6 mm (T_f/T_c <0.3 are classified as "thin facesheets" and facesheets with thicknesses greater than 6 mm (T_f/T_c >0.3) are classified as "thick facesheets".

As previously described, the Hashin damage model for fiber-reinforced composites takes into account tensile and compressive damage. Figures 9 and 11 show the distribution of damage parameter F_m^t in the last ply in the composite layup in facesheets-1 and 2. The minimum value is 0 which denotes the undamaged state and the maximum value is 1 which denotes the completely damaged state. Note that what is shown is not the cumulative damage in an entire facesheet. Rather, the figures show damages in the ply in each of the facesheets that is farthest away from the front face of the sandwich specimen. The distribution and severity of damage facilitate comparison of the results for different T_f/T_c ratios under identical loading conditions. Figure 9 shows the distribution of tensile damage in the matrix for the last ply of the facesheets 600 μs after onset of deformation in a sandwich plate with a facesheet thickness of 1 mm (T_f/T_c=0.05). The load intensity is I=18 kPa·s.

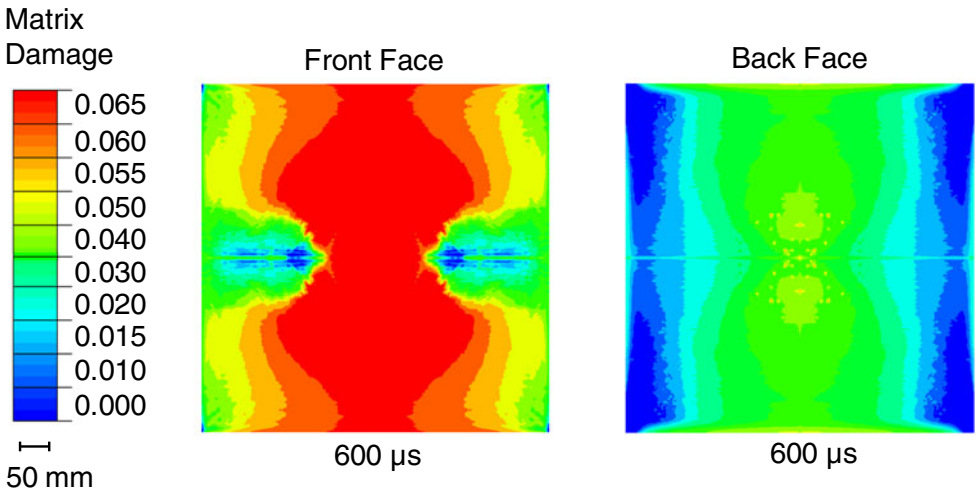

Fig. 9 Distributions of tensile damage in the matrix of the facesheets at t=600 μs. T_f/T_c=0.05 and I=18 kPa·s for the ply in the composite layup farthest away from the front (impact) face of the sandwich specimen. The plies shown are oriented vertically

Damage in the front sheet (facesheet 1) is more severe and is dependent on fiber orientation. Maximum damage occurs close to the loading area and spreads outward in later stages of the loading event. Figure 10 shows the corresponding distributions of equivalent plastic strain at three different times for this structure sandwich. The arrival of the load pulse at the target is taken as t=0. Core compression occurs immediately after the onset of loading. Facesheet 2 starts to deform at t=100 μs and has acquired significant momentum by t=500 μs. Since the facesheets are thin, core crushing is highly localized and the rate of deformation is highly non-uniform in the core. Significant core-facesheet debonding is observed at late stages of the deformation.

Figure 11 shows the tensile damage in the matrix for the final ply of the facesheets in a sandwich structure with a facesheet thickness of 8 mm (T_f/T_c=0.4). While the damages in facesheet 1 for both T_f/T_c=0.05 (Fig. 9) and T_f/T_c=0.4 (Fig. 11) are similar, the damages in facesheet 2 are quite different, with the damage for T_f/T_c=0.4 being much lower than that for T_f/T_c=0.05. Beyond T_f/T_c=0.4, there is essentially no further improvement in damage resistance. This observation is supported by the analysis of deflections discussed in next section. Figure 12 shows the corresponding distributions of equivalent plastic strain for the sandwich plate in Fig. 11. Core deformation is more spread out relative to what is seen in Fig. 10 (thinner facesheets) and the motion of facesheet 2 starts at a later time of t=140 μs compared with what is seen in Fig. 10. Facesheet 2 has acquired significant momentum by t= 500 μs. Figures 10 and 12 show that, as T_f/T_c increases, core compression becomes less localized and the deformation in the core becomes more uniformly distributed. Thicker facesheets also delay the onset of deformation of facesheet 2 and the momentum transfer into facesheet 2. After the core is fully compressed, the deformation of the structure occurs primarily through bending. Facesheet 1 is in compression and facesheet 2 is in tension. The damage in the facesheets (through matrix cracking and fiber breakage which are considered phenomenologically) provides one mechanism for energy dissipation. Like damage in the facesheets, core-facesheet debonding is more severe for thin facesheets.

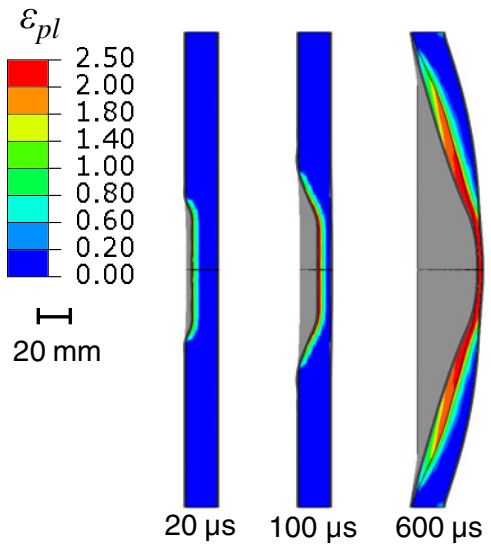

Fig. 10 Distributions of equivalent plastic strain in the core at different times. T_f/T_c=0.05 and I=18 kPa·s

Deflection

The duration of loading on the target is approximately 250 μs. The displacements at the center of the structures are used to quantify deflection and core compression. In particular, the displacements at the center of the front and back facesheets (Δ) at 600 μs after the onset of loading are analyzed. The deflections are normalized with the side length (L) of the sandwich plates. Figure 13 shows that Δ/L increases with I and decreases with the ratio between the thickness of the facesheets and the thickness of the core

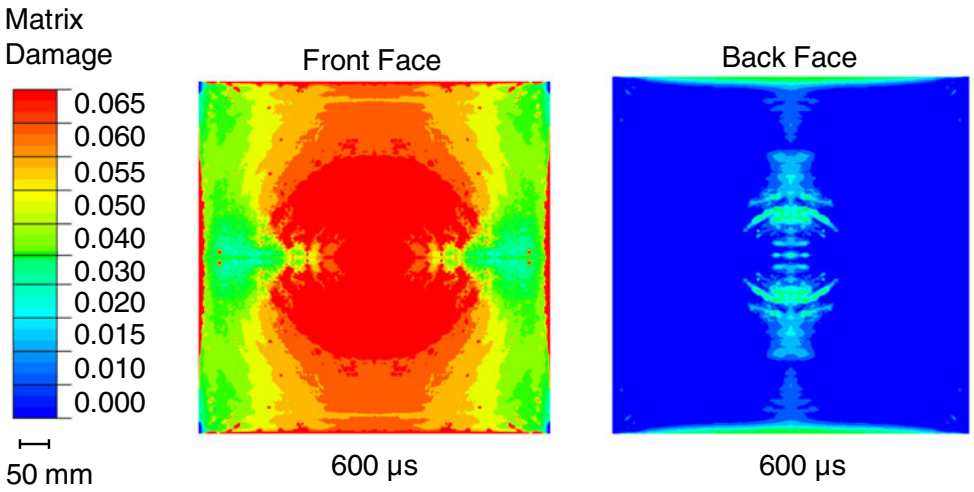

Fig. 11 Distributions of tensile damage in the matrix of the facesheets at t=600 μs. T_f/T_c=0.4 and I=18 kPa·s for the ply in the composite layup farthest away from the front (impact) face of the sandwich specimen. The plies shown are oriented vertically

(T_f/T_c) [and therefore decreases with the areal mass of sandwich plates (M)]. The deflection of facesheet 2 is generally lower than that of facesheet 1, due to core compression. As T_f/T_c increases, the decreases in deflections are monotonic. At low impulse magnitudes (I< 12 kPa·s), increasing facesheet thickness does not provide significant reductions in the deflections. As the impulse magnitude increases, the difference between the responses of structures with low T_f/T_c and the responses of those with high T_f/T_c becomes pronounced. For impulse magnitudes above 12 kPa·s, structures with high T_f/T_c values show markedly lower deflections. For example at I=18, 30, 42 kPa·s, as T_f/T_c increases from 0.01 to 0.36, Δ/L decreases by approximately 56%. If T_f/T_c increases from 0.6 to 1, Δ/L decreases by only ~5%. At all impulse magnitudes, no appreciable reduction in the deflection of facesheet 1 is seen for T_f/T_c>0.6. The deflections of facesheet 2 shown in Fig. 13(b) are generally lower than the deflections of facesheet 1 but exhibit the same trend seen in Fig. 13(a). Figure 14 shows Δ/L as a function of impulse (I) for different values of T_f/T_c.

Overall, increasing the relative thickness of the facesheets up to a certain value (T_f/T_c=0.6) can significantly decrease the deformation of the structures. Increases beyond this value yields no obvious benefit in terms of structural rigidity. Since the overall weight of the structures is one of the most important aspects in naval structural design, this finding points to a design criterion useful for relevant systems.

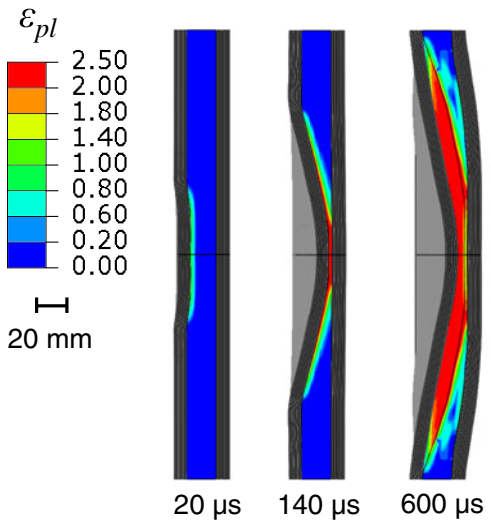

Fig. 12 The distributions of equivalent plastic strain in the core at different times. T_f/T_c=0.4 and I=18 kPa·s

Energy Absorption

Energy dissipation in glass-fiber reinforced composites is in the form of matrix cracking, fiber breakage and delamination. In the current analysis, only matrix and fiber damages are considered. Energy absorption in the core is in the form of permanent core compression which accounts for the largest portion of overall energy dissipated. For the load conditions analyzed, the primary mode of core deformation is compression with very small amounts of stretching at the supports. Therefore, taking full advantage of core compression is important. Calculations of the dissipated work associated with different deformation and damage mechanisms are described in [30]. The dissipation in each component of the structure (facesheet-1, facesheet-2, core, and core-facesheet interfaces) is tracked. The energy dissipated in the entire structure is the sum of the dissipation in the components. The dissipation in the facesheets is due to damage in the matrix and fibbers of the composite plies as described by the Hashin model. The

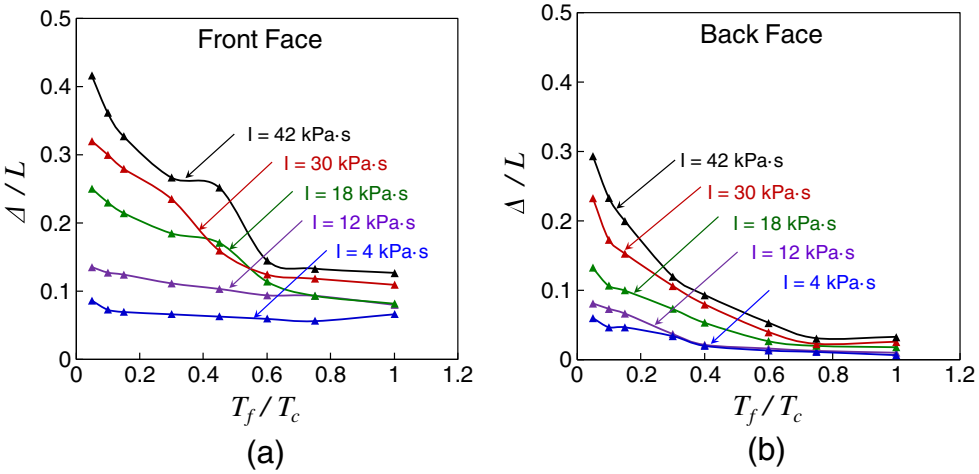

Fig. 13 Normalized displacement as a function of T_f/T_c for (**a**) front facesheet (*facesheet 1*) and (**b**) back facesheet (*facesheet 2*)

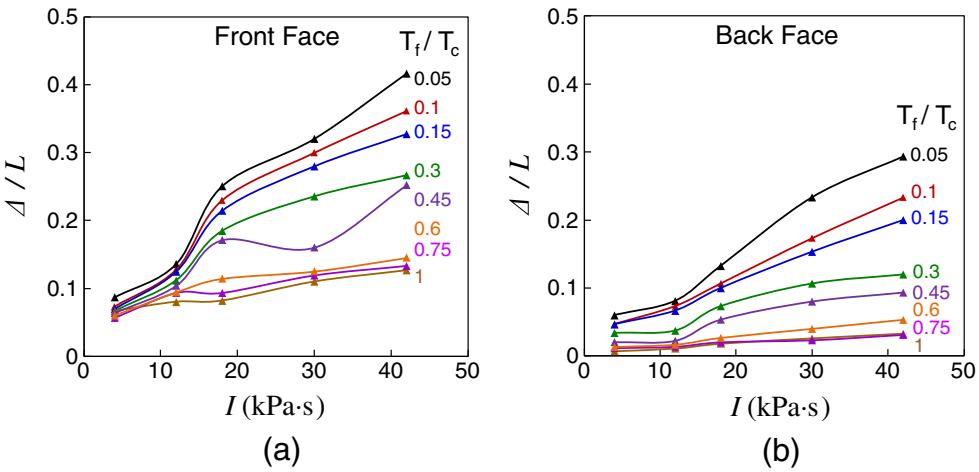

Fig. 14 Normalized displacement as a function of impulse magnitude for (**a**) front facesheet (*facesheet 1*) and (**b**) back facesheet (*facesheet 2*)

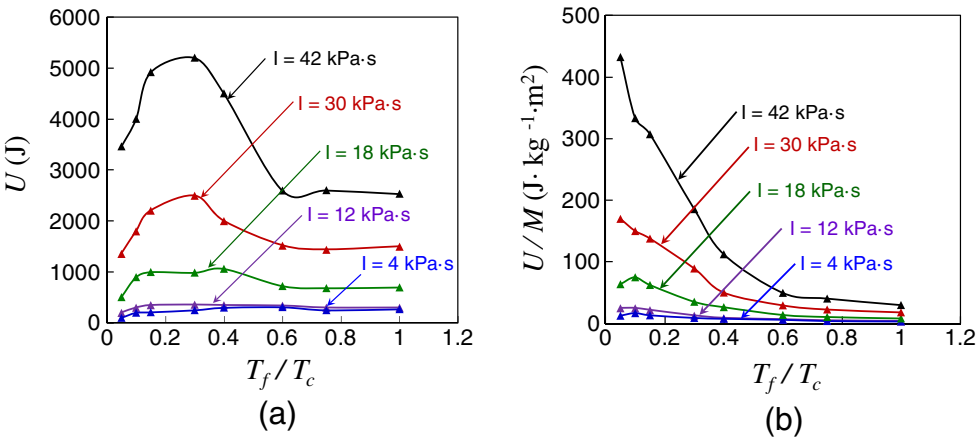

Fig. 15 (**a**) Energy dissipated in the entire structure as a function of T_f/T_c, (**b**) energy dissipated per unit areal mass as a function of T_f/T_c

dissipation in the foam core is due to inelastic, pressure-dependent deformation of the core material (core compression). The dissipation along core-facesheet interfaces is due to interfacial damage and fracture. Since the dissipation along core-facesheet interfaces is very small compared with the dissipation in the core and the facesheets for the conditions analyzed, interfacial dissipation is not explicitly discussed here. Figure 15(a) shows the total energy dissipated in the structure (U) as a function of T_f/T_c. For thin facesheets ($T_f/T_c<0.15$), the core compression is highly localized to the load area, leaving large portions of the core relatively intact or underused. For $0.15 < T_f/T_c < 0.45$, the facesheets are rigid enough to distribute core compression over a larger area, whereby achieving maximum energy dissipation. For $T_f/T_c>0.6$, no further improvement in energy dissipation can be gained at all impulse magnitudes, since the core is already fully utilized. An interesting aspect of this plot is that U reaches a maximum at a certain value of T_f/T_c, indicating that there is an optimum thickness ratio (approximately $T_f/T_c=0.2$–0.3) for maximizing energy dissipation. This maximum becomes more obvious at higher load intensities.

Figure 15(b) shows the energy dissipated per unit areal mass (U/M) as a function of T_f/T_c for different load intensities. As the T_f/T_c increases, U/M decreases significantly and eventually levels off at around $T_f/T_c=0.6$. The facesheets significantly increase the weight of the structure but provide lesser capability for energy dissipation.

Performance of Sandwich Core

By keeping the dimensions and material properties of the core the same for all cases, we can assess the performance of the core at different facesheet thicknesses. Figure 16 shows the energy dissipated per unit areal mass (U/M) in the core as a function of T_f/T_c at different impulse magnitudes. The results are in general agreement with those in Fig. 15(a), because the core is responsible for a significant amount of the energy dissipated in the structures.

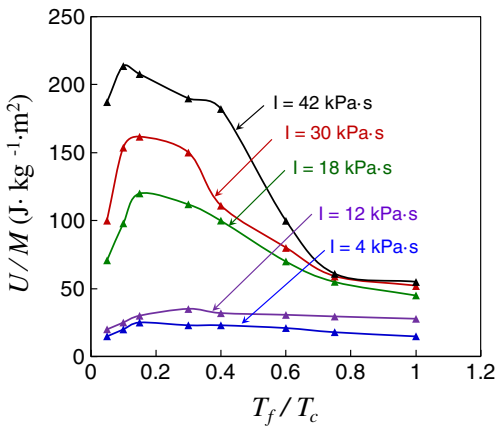

Fig. 16 Energy dissipated per unit areal mass as a function of T_f/T_c for the Divinycell H100 foam core. Note that areal mass of core is the same in all calculations

Desirable Structural Configurations

The desired attributes for a sandwich structure is high energy dissipation capacity and high stiffness (small deflections). For energy dissipation, we consider the energy dissipated per areal mass. For stiffness, we consider maximum deflection of the structure. Figures 13, 14 and 15 show that there is practically no performance benefit for structures with $T_f/T_c>0.6$. Figures 15(a) and 16 show that the highest energy dissipation capacity occurs for $0.15 < T_f/T_c < 0.4$. Figure 13 shows increases in facesheet thickness are most effective for $0.05 < T_f/T_c < 0.3$. Accounting for both factors, the most desirable range for facesheet thickness is T_f/T_c between 0.15 and 0.4 for a given core configuration.

Conclusions

The responses to underwater impulsive loads of composite sandwich plates consisting of glass-fiber reinforced epoxy facesheets and PVC foam core with different facesheet-thickness-to-core-thickness ratios are analyzed. The configuration studied is that used in experiments being carried out in the Underwater Shocking Loading Simulator recently developed at Georgia Tech. For comparison purposes, all material properties and core dimensions are kept constant. A fully dynamic 3D finite element model is developed for the experimental configuration, accounting for impulsive loading generation and the dynamic response processes of the structure and water. Deformation and failure mechanisms considered are core crushing, facesheet damage, and core-facesheet separation and contact. Calculations show the distinct response regimes of the structures, as measured by energy dissipated and the maximum deflection. It is found that under the loading conditions and for the material systems analyzed, there is a range of facesheet thickness in which planar sandwich structures offer the best performance. Specifically, structures with facesheet-thickness-to-core-thickness ratios between 0.15 and 0.4 provide the most efficient use of material in terms of both energy dissipation capacity and rigidity. The insight gained here provides guidelines for the design of structures for which response to water-based impulsive loading is an important consideration. It is important to note that the analysis reported here concerns only one structural

configuration, one combination of core and facesheet materials, and one core size. More extensive analyses and experimental verification are needed to determine the applicability of the findings to sandwich structures of different geometries, sizes and materials.

Acknowledgement The authors gratefully acknowledge support by the Office of Naval Research through grant numbers N00014-09-1-0808 and N00014-09-1-0618 (program manager: Dr. Yapa D. S. Rajapakse). Calculations are carried out on the HPC cluster in the DPRL at Georgia Tech.

References

1. Zenkert D (1995) An introduction to sandwich construction. West Midlands U.K., Engineering Materials Advisory Services Ltd
2. Plantema F (1996) Sandwich construction. Wiley, New York
3. Allen H (1969) Analysis and design of structural sandwich panels. Pergamon Press, Oxford
4. Steeves CA, Fleck NA (2004) Collapse mechanisms of sandwich beams with composite faces and a foam core, loaded in three-point bending. Part II: experimental investigation and numerical modelling. Int J Mech Sci 46(4):585–608
5. Tagarielli VL, Deshpande VS, Fleck NA (2007) The dynamic response of composite sandwich beams to transverse impact. Int J Solid Struct 44(7–8):2442–2457
6. Schubel PM, Luo JJ, Daniel IM (2007) Impact and post impact behavior of composite sandwich panels. Compos Appl Sci Manuf 38(3):1051–1057
7. Nemes JA, Simmonds KE (1992) Low-velocity impact response of foam-core sandwich composites. J Compos Mater 26(4):500–519
8. Mines RAW, Worrall CM, Gibson AG (1994) The static and impact behavior of polymer composite sandwich beams. Compos 25(2):95–110
9. Abot JL, Daniel IM (2001) Composite sandwich beams under low velocity impact. Proc. of AIAA Conf., Seattle
10. Schubel PM, Luo JJ, Daniel IM (2005) Low velocity impact behavior of composite sandwich panels. Compos Appl Sci Manuf 36(10):1389–1396
11. Xue ZY, Hutchinson JW (2003) Preliminary assessment of sandwich plates subject to blast loads. Int J Mech Sci 45(4):687–705
12. Xue ZY, Hutchinson JW (2004) A comparative study of impulse-resistant metal sandwich plates. Int J Impact Eng 30(10):1283–1305
13. Liang YM et al (2007) The response of metallic sandwich panels to water blast. J Appl Mech Trans Asme 74(1):81–99
14. Wei Z et al (2008) The resistance of metallic plates to localized impulse. J Mech Phys Solid 56(5):2074–2091
15. Tekalur SA, Bogdanovich AE, Shukla A (2009) Shock loading response of sandwich panels with 3-D woven E-glass composite skins and stitched foam core. Compos Sci Tech 69(6):736–753
16. Espinosa HD, Lee S, Moldovan N (2006) A novel fluid structure interaction experiment to investigate deformation of structural elements subjected to impulsive loading. Exp Mech 46(6):805–824
17. Horacio D, Espinosa DG, Latourte F, Ravi S (2010) Bellur-Ramaswamy Failure modes in solid and sandwich composite panels subjected to underwater impulsive loads. 9th International Conference on Sandwich Structures, ICSS9
18. Wei Z et al (2007) Analysis and interpretation of a test for characterizing the response of sandwich panels to water blast. Int J Impact Eng 34(10):1602–1618
19. LeBlanc J, Shukla A (2010) Dynamic response and damage evolution in composite materials subjected to underwater explosive loading: an experimental and computational study. Compos Struct 92(10):2421–2430
20. Arora H, Hooper P, Dear JP (2010) Blast and other high rate loading composite sandwich materials. 9th International Conf on Sandwich Structures (ICSS-9), Ravichandran, G. ed, California Institute of Technology, Pasedena, USA (June 2010), Key-note paper MA3.1
21. Saha MC, Kabir ME, Jeelani S (2008) Enhancement in thermal and mechanical properties of polyurethane foam infused with nanoparticles. Mater Sci Eng a-Struct Mater Prop Microstruct Process 479(1–2):213–222
22. Chakravarty U et al (2003) Strain rate effects on sandwich core materials: an experimental and analytical investigation. Acta Mater 51(5):1469–1479
23. Tagarielli VL, Deshpande VS, Fleck NA (2008) The high strain rate response of PVC foams and end-grain balsa wood. Compos Part B-Eng 39(1):83–91
24. Mouritz AP (1996) The effect of underwater explosion shock loading on the flexural properties of GRP laminates. Int J Impact Eng 18(2):129–139
25. Mouritz AP, Saunders DS, Buckley S (1994) The damage and failure of Grp laminates by underwater explosion shock loading. Compos 25(6):431–437
26. McShane GJ et al (2008) Dynamic rupture of polymer-metal bilayer plates. Int J Solid Struct 45(16):4407–4426
27. Dharmasena K et al (2009) Dynamic response of a multilayer prismatic structure to impulsive loads incident from water. Int J Impact Eng 36(4):632–643
28. DIAB Inc., S.D., DeSoto, Texas 75115, USA http://www.diabgroup.com/europe/literature/e_pdf_files/man_pdf/H_man.pdf Accessed 5 May 2011
29. Zhang J et al (1998) Constitutive modeling of polymeric foam material subjected to dynamic crash loading. Int J Impact Eng 21 (5):369–386
30. Hibbit, Karlsson, and Sorensen (2009) Abaqus/Explicit User's Manual, Version 6.9
31. Deshpande VS, Fleck NA (2000) Isotropic constitutive models for metallic foams. J Mech Phys Solid 48(6–7):1253–1283
32. Hashin Z (1980) Failure criteria for unidirectional fiber composites. J Appl Mech Trans Asme 47(2):329–334
33. Taylor GI (1941) The pressure and impulse of submarine explosion waves on plates. The scientific papers of G I Taylor, vol. III. Cambridge, Cambridge University Press, pp 287–303
34. Camanho PP, Davila CG, de Moura MF (2003) Numerical simulation of mixed-mode progressive delamination in composite materials. J Compos Mater 37(16):1415–1438
35. Advanced Composites Group Inc, S., 129th East Avenue, Tulsa, Oklahoma, 74134, USA http://www.advanced-composites.co.uk/data_catalogue/catalogue%20files/pds/PDS1154_VTM260_Issue7.pdf Accessed 5 May 2011.